American Journal of Engineering and Applied Sciences

Original Research Paper

Optoelectronic Characterisation of Silicon and CIGS Photovoltaic Solar Cells

[1]Afonso Ravasco, [2]Ricardo A. Marques Lameirinhas, [2]Catarina Pinho Correia Valério Bernardo and [3]João Paulo N. Torres

[1]Instituto de Telecomunicações, Lisbon, Portugal
[2]Department of Electrical and Computer Engineering, Universidade de Lisboa-Instituto Superior Técnico, Portugal
[3]Academia Militar/CINAMIL, Av. Conde Castro Guimarães, Amadora, Portugal

Article history
Received: 13-11-2023
Revised: 20-11-2023
Accepted: 22-11-2023

Corresponding Author:
Ricardo A. Marques Lameirinhas
Department of Electrical and Computer Engineering, Universidade de Lisboa-Instituto Superior Técnico, Portugal
Email: ricardo.lameirinhas@tecnico.ulisboa.pt

Abstract: Throughout these years, many materials have been subjected to tests and experiments, creating several photovoltaic technologies and generations. In this article, some of these generations are compared, namely silicon and Copper Indium Gallium di-Selenide (CIGS), in order to characterize both materials in an optoelectronic way. Using a 2D solar cell PIN model using COMSOL software, both materials are tested, obtaining the responsivity and the I(P) curves. In addition, experimental tests are also conducted, in order to have real results to compare. Additionally, Scanning Electron Microscopy (SEM) was performed to analyze the morphology of photovoltaics inside layers. The obtained results show that Si solar cells present properties close to those predicted by the 2D model, in opposition to the CIGS. That difference was found to be the amount of generated current and more, gallium concentration has a remarkable effect on the CIGS photovoltaics real performance.

Keywords: Optoelectronic Devices, Photovoltaic Technology, Renewable Energy, Semiconductors

Introduction

Solar technology has come a long way since the design of the first crystalline silicon solar cell back in 1954 in the Bell Laboratories, USA, registering an efficiency of about 4%. However, the first idea of a solar cell or photovoltaic conversion might have been born in 1839, by Alexandre Becquerel, when he detected photogenerated current on silver and platinum electrodes exposed to the sun radiation (Battaglia *et al*., 2016; Marques Lameirinhas *et al*., 2022; Nain and Kumar, 2021; Olchowik *et al*., 2023; Pinho Correia Valério Bernardo *et al*., 2023).

Solar cell technology has been evolving over the last 50 years. There have been many types of photovoltaic devices and technologies throughout the years, so to sort out these technologies, they have been inserted into generations, according to their materials' properties and their evolution over time as well. The most common solar cells available in the market belong to the first generation, single band-gap solar cells, comprised of germanium and the most dominating material in the PV market, silicon. Silicon is one of the most abundant materials on Earth, accounting for about 25% of its crust, as well as being very cheap and it is easy to produce (Olchowik *et al*., 2023; Dos Santos Castilho *et al*., 2021; De Melo Cunha *et al*., 2022). The second generation is based on thin-film technologies. This technology was introduced to reduce the used material from the previous solar cell technologies, achieving layers as thin as tens of micrometers or even nanometres. This layer is deposited on a layer of substrate such as glass, stainless steel, or plastic and, due to the thinness of this layer, it is possible to build flexible devices that can have many applications. Some examples of second-generation materials are amorphous silicon, gallium arsenide and Copper Indium Gallium di-selenide (CIGS) (Isabela *et al*., 2021; Torres *et al*., 2023a-b; Palit and Hussain, 2018; Jalali *et al*., 2023; Kant and Singh, 2022). There is also the third generation, which includes non-based silicon solar cell materials, such as Perovskite Solar Cells (PSC), Organic Solar Cells (OSC) and Dye-Sensitized Solar Cells (DSSC). These types of photovoltaic technology use a combination of

organic and inorganic materials to generate electron-hole pairs, hence creating a photovoltaic effect throughout several layers. Despite some of these cells still struggling to provide good efficiency, significant progress on the power conversion efficiency of these cells is being made, guaranteeing a promising future for this technology (Akinoglu *et al*., 2021; Soga, 2006; Sun *et al*., 2022; Pastuszak and Węgierek, 2022).

This research work aims to create a solar cell's 2D model, which is used to be an approximation of an actual solar cell, mainly focused on the absorbing layer, responsible for generating electron-hole pairs, using two different photovoltaic generations of solar cells. The 2D model is designed with the COMSOL multi-physics software and originally the 2D model. Lastly, real case scenarios will also be taken into consideration, in order to study the materials more extensively. To complement this experimental component, an SEM analysis will be performed as well, mainly to determine the inside layers of the studied panels. Two different materials are going to be analyzed in this study: CIGS and Silicon. On the one hand, silicon, representing the first generation of solar cells, is known for its market domination and is the lead material in solar panel production. It is known to produce high efficiencies and have a wide absorption range. On the other hand, CIGS represents the second generation, specifically the thin-film technology. Thin films are known to use much less material than other solar cells and recently have achieved very high results. However, indium is a rare element in the Earth and consequently, the future of CIGS technology is limited by it.

Simulation

To analyze and perform different simulations on the behavior of solar cell materials, a 2D PIN solar cell model is considered.

A PIN structure consists of 3 layers of semiconductors, a p-type layer, an n-type layer and an intrinsic layer (i-layer). By adding this i-layer, it is possible to reduce surface recombination, which has an influential role in the generated current of a solar cell, especially in small areas (Imran *et al*., 2018; Amraoui *et al*., 2022). The i-layer also provides a wider depletion region, increasing the minority carrier diffusion length as well as strengthening the charge carrier lifetime (which reduces recombination) (Amraoui *et al*., 2022; Alizade and Ghadimi, 2019).

The 2D model is designed in COMSOL multi-physics software, as illustrated in Fig. 1, having constant illumination from the top. The p-layer and the n-layer are both composed of a heavily doped contact at the top (p+) and bottom (n+) of the cell, respectively. In addition, there are also larger p and n-doped areas that contain less dopant (about 100 times less). This second layer is added in order to have an easier diffusion of the carriers, throughout the solar cell, in order to generate the intrinsic layer in between.

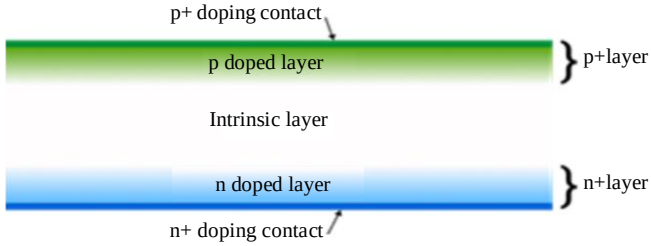

Fig. 1: Illustration of the used solar cell PIN model

For the two materials under analysis, which concern the CIGS', it is important to note that the CIGS solar cell is composed of many other layers, but it acts as the p-type material of the entire cell. Besides that, in CIGS, depending on the gallium's concentration, the band gap and the electron affinity vary. In this particular case, for the n-layer section of the CIGS PIN model, the donor density used will be equal to the doping of the CDS buffer layer, simulating the interface between CIGS and the buffer. The gallium-dependent values for CIGS offer the possibility to conduct a deeper study of the responsivity and current-power relationship for different concentrations of CIGS (Isabela *et al*., 2021; Paulson *et al*., 2003; Layachi *et al*., 2023; Nicolás-Marín *et al*., 2022).

In the literature, previous studies of the CIGS material specify gallium concentration values, which are used to obtain the stated results presented in Table 1 (Isabela *et al*., 2021; Paulson *et al*., 2003; Layachi *et al*., 2023).

Responsivity

In this research study, the responsivity of the solar cells is obtained. Different solar cell materials are tested with the PIN model, with the primary goal of validating the model, by checking how similar the responsivity curves match the already known curves of the referred materials.

Figure 2 shows the results for the silicon solar cell. Based on the obtained results, silicon has an absorption range starting around 370 nm, which means that this cell cannot work properly for UV/violet radiation. However, it is possible to see a steady rise in the materials' responsivity, generating higher currents throughout the whole visible spectrum. Moreover, the silicon response has its peak at 1030 nm (infrared radiation), reaching a maximum of 0.778 µA/W.

Table 1: Band gap and electron affinity values for each percentage of gallium in CIGS (Palit and Hussain, 2018)

Material	*X*	Bandgap (eV)	Electron affinity (eV)
CIS	0.00	1.023	4.57
CIGS-31	0.31	1.208	4.25
CIGS-45	0.45	1.351	4.10
CIGS-66	0.66	1.457	3.93
CGS	1.00	1.771	3.87

[1]To $x = 0$, the cell has no percentage of gallium, known as CIS. For $x = 100$, the cell has no indium, therefore CGS

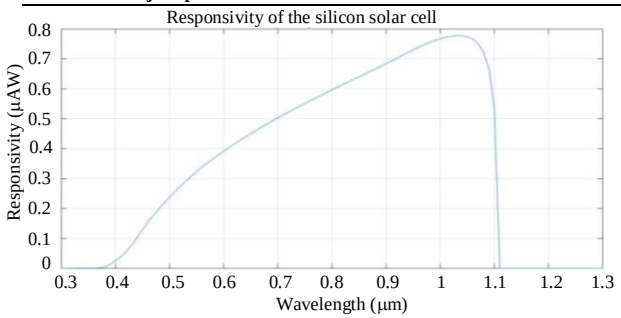

Fig. 2: Responsivity of silicon

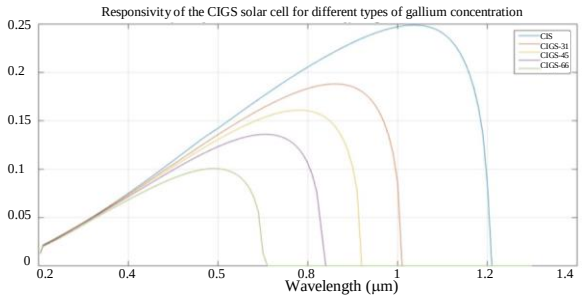

Fig. 3: Responsivity of CIGS

For the CIGS responsivity, presented in Fig. 3, the gallium concentration is considered, due to its influential role, when determining certain material properties. Through the analysis of Fig. 3, it is possible to observe a decrease in the wavelength value where the responsivity peak is reached, as well as the peak's value itself, as the concentration of gallium increases. This is an expected result since the increase of gallium within the CIGS cell increases its band gap, thus narrowing its absorption range. The responsivity peak value also decreases when the gallium concentration is increased, which is a consequence of the previous analysis (Isabela *et al*., 2021). According to Fig. 3, CIS has a maximum responsivity of 0.25 μA/W at 1.023 μm; CIGS-31 has a maximum responsivity of 0.182 μA/W at 0.855 μm; CIGS-45 has a maximum responsivity of 0.156 μA/W at 0.773 μm; CIGS-66 has a maximum responsivity of 0.132 μA/W at 0.703 μm; CGS has a maximum responsivity of 0.098 μA/W at 0.591 μm.

Regarding the responsivity values, the CIGS solar cell presents very low values compared to the silicon's. In theory, both results should be relatively close to each other. Since a CIGS cell is composed of three more layers (minimum), each one with its own band gap and doping density, it could explain why the generated current per incident power is so low, as the CIGS absorber layer requires the presence of the other layers in order to unlock its full potential. However, the theoretical results do not reveal the concentration of gallium, but the previous reason can also play a crucial role in widening the absorption band since the theoretical CIGS has almost the same absorption range as the simulated CIS. Moreover, the obtained results are for standard active and absorbent areas. This means that, for higher areas, the responsivity value should be higher too. However, all these simulations are performed for the same conditions. Then, it is possible to normalize the obtained values.

With the analysis carried out, it is possible to conclude that for the same structure, silicon solar cells should generate more current per watt of incident radiation than CIGS.

Current-Power Relation

In order to verify the linearity between the generated current of the cell, IL and the incident radiation power, pin, it is possible to perform the current-power relation. To better represent the correlation of current and power, it is used the poly fit function from MATLAB to find the equation that best fits the data, which is better described by the expression 1:

$$P(x) = p_n x_n + p_{n-1} x_{n-1} + p_{n-2} x_{n-2} + \ldots + p_0 \qquad (1)$$

To achieve better results of the I(*P*) characteristics, specific wavelengths were taken into consideration, as shown in Table 2.

Figure 4 shows the I(*P*) curve for the silicon solar cell. In this figure, it is possible to verify that, for all the studied wavelengths, the generated current from the solar cell has a linear relation with the incident light's power. In the UV wavelength, the absorption of the silicon cell is very close to zero, since the responsivity for silicon solar cells at the UV mark is practically null, as previously verified. As the wavelengths increase, the slope of each function increases as well, since the responsivity of silicon reaches its peak at 1030 nm (Fig. 2), which corresponds to the IR region.

For each wavelength, the curve that best fitted the data points was plotted and, taking into account Eq. 1, the obtained coefficients for the silicon solar cell are presented in Table 3.

For the CIGS case, the gallium concentration has to be considered. Since it is a more complex material than silicon, some differences are expected in the I(P) characteristics.

Table 2: Selected wavelengths to study the I(P) curves

Spectrum region	UV	Blue	Green	Orange	IR
Wavelength (nm)	300	420	550	690	800-1100

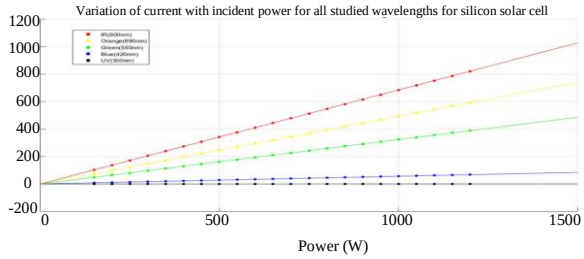

Fig. 4: I(P) curve for silicon solar cell

Table 3: Extracted coefficients from the poly fit function of the silicon solar cell I(P) data points

	UV (300 nm)	Blue (420 nm)	Green (550 nm)	Orange (690 nm)	IR (900 nm)
P1	1.04×10^{-4}	0.057	0.324	0.493	0.685
P0	5.87×10^{-7}	-3.09×10^{-5}	-0.001	-0.003	-0.006

Table 4: Coefficients of the 3rd order polynomial expression that best fitted CGS, for the different wavelengths

	UV (300 nm)	Blue (420 nm)	Green (550 nm)	Orange (690 nm)	IR (900 nm)
P3	1.906×10^{-9}	3.598×10^{-9}	5.69×10^{-9}	-3.588×10^{-9}	-
P2	-5.998×10^{-6}	-1.409×10^{-5}	-2.132×10^{-5}	-1.411×10^{-5}	-
P1	0.0348	0.0609	0.083	0.047	-
P0	1.0450	1.5290	1.973	1.200	-

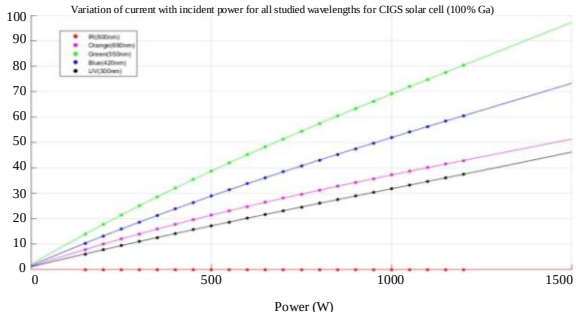

Fig. 5: I(P) curve for the CGS solar cell

Figure 5 shows the I(P) characteristic of the CGS solar cell.

The CGS solar cell holds the smallest responsivity window and, as can be seen, in the IR wavelength, the absorption of the solar cell is null. For the smallest wavelengths, around the UV mark, the CGS material presented has a linear current increase with the power. Besides that, once the wavelength starts increasing, the I(P) function starts to drift away from its linear shape, assuming a slightly curved shape. This small curve shape starts getting a bit more noticeable as the wavelength increases. Along with the curving, the slope begins to increase as well, which is a natural response of the material's responsivity.

Nevertheless, once the wavelength for the maximum peak of current is surpassed (590 nm), the produced current is decreased. Therefore, the green radiation can produce higher output currents, as can be seen in Fig. 5. Table 4 presents all the obtained coefficients of the equation that best fits CGS for all wavelengths under analysis.

For CIGS-66 and CIGS-45 solar cells, the I(P) curves are presented in Figs. 6-7. In both cases, the orange radiation is the one that presents the highest generated current of the remaining wavelengths under study, although the IR radiation for the CIGS-45 has a higher absorption, which means that it will not pass through the solar cell nor reflect. Tables 5-6 present the coefficients for each curve that best fitted CIGS-66 and CIGS-45 for the different wavelengths, respectively.

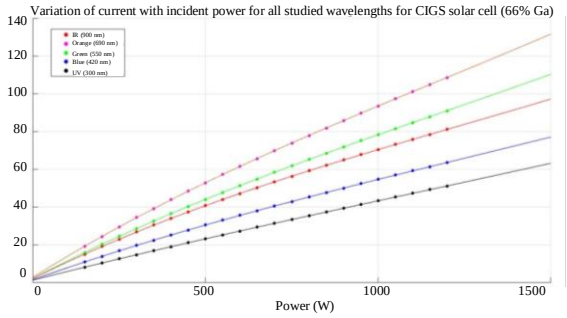

Fig. 6: I(P) curve for the CIGS-66 solar cell

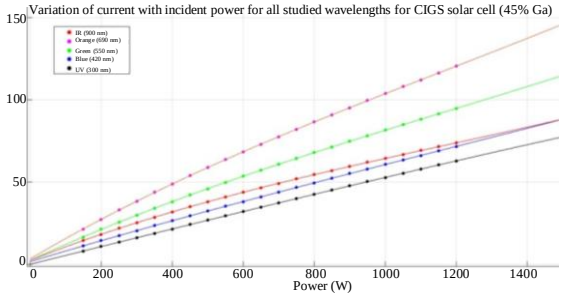

Fig. 7: I(P) curve for the CIGS-45 solar cell

Table 5: Coefficients of the 3rd order polynomial expression that best fitted CIGS-66, for the different wavelengths

	UV (300 nm)	Blue (420 nm)	Green (550 nm)	Orange (690 nm)	IR (900 nm)
P3	2.063×10^{-9}	4.094×10^{-9}	7.16×10^{-9}	9.251×10^{-9}	8.038×10^{-9}
P2	-6.639×10^{-6}	-1.569×10^{-5}	-2.595×10^{-5}	-3.283×10^{-5}	2.991×10^{-5}
P1	0.047	0.065	0.095	0.1143	0.090
P0	1.311	1.560	2.259	2.7900	2.177

Table 6: Coefficients of the 3rd order polynomial expression that best fitted CIGS-45, for the different wavelengths

	UV (300 nm)	Blue (420 nm)	Green (550 nm)	Orange (690 nm)	IR (900 nm)
P3	-7.805×10^{-10}	2.44×10^{-9}	7.728×10^{-9}	-1.077×10^{-8}	9.008×10^{-9}
P2	-3.24×10^{-7}	-8.153×10^{-6}	-2.766×10^{-5}	-3.744×10^{-5}	-3.187×10^{-5}
P1	0.0539	0.0649	0.0991	0.127	0.085
P0	-0.0253	1.6320	2.3820	3.268	2.433

Regarding CIGS-31, which I(P) curve is presented in Fig. 8, it is possible to verify that the IR radiation has surpassed the orange radiation when it comes to the generated current, achieving a maximum of 143.7 µm. Nonetheless, no changes were found in the curvature of the I(P) function for each specific wavelength from the previous results. For the different wavelengths, Table 7 states the coefficients for the curve that best fits the cell's curve.

With the CIS solar cell, presented in Fig. 9, the responsivity range reaches its maximum, which means that the maximum current peak surpassed the maximum wavelength in the study. Because of that, it was increased the study range for the IR region, so the 1100 nm mark was added. This increase in the IR region could prove

that as the wavelength rises the non-linearity of CIGS increases further since it is possible to get almost the same maximum current for both 900 and 1100 nm wavelengths. All the obtained coefficients for the CIS solar cell are presented in Table 8 for the different solar cells.

Once all the I(P) curves have been obtained, it is possible to conclude that a relationship of the non-linearity to the increase of wavelength exists, since most of the non-linear results occur above the green radiation. This non-linearity can also be spotted in an earlier stage, more specifically in the blue radiation for CGS because the absorption range is very small.

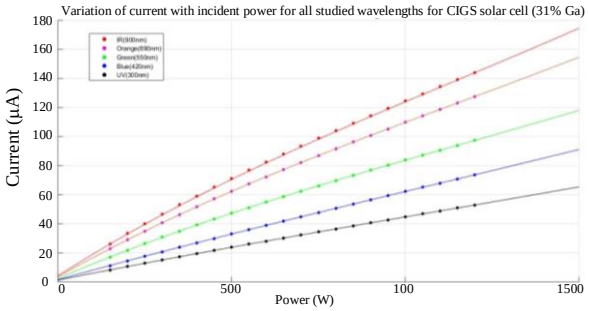

Fig. 8: I(P) curve for the CIGS-31 solar cell

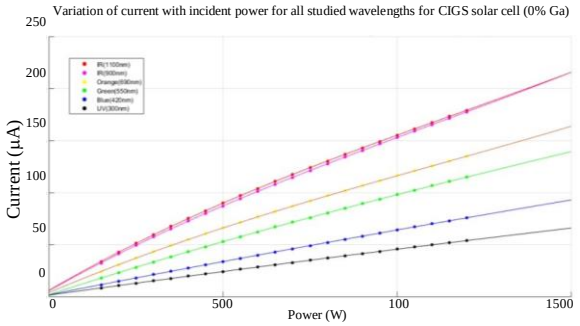

Fig. 9: I(P) curve for the CIS solar cell

Table 7: Coefficients of the 3rd order polynomial expression that best fitted CIGS-31, for the different wavelengths

	UV (300 nm)	Blue (420 nm)	Green (550 nm)	Orange (690 nm)	IR (900 nm)
P3	1.997×10^{-9}	2.456×10^{-9}	8.13×10^{-9}	1.169×10^{-8}	1.363×10^{-8}
P2	-6.446×10^{-6}	-7.988×10^{-6}	-2.888×10^{-5}	-4.023×10^{-5}	-4.770×10^{-5}
P1	0.048	0.066	0.102	0.135	0.154
P0	1.284	1.622	2.468	3.557	4.245

Table 8: Coefficients of the 3rd order polynomial expression that best fitted CIS, for the different wavelengths

	UV (300 nm)	Blue (420 nm)	Green (550 nm)	Orange (690 nm)	IR (900 nm)	IR (1100 nm)
P3	1.943×10^{-9}	2.414×10^{-9}	2.7×10^{-9}	1.270×10^{-8}	1.722×10^{-8}	1.838×10^{-8}
P2	-6.279×10^{-6}	-7.846×10^{-6}	-1.571×10^{-5}	-4.32×10^{-5}	5.749×10^{-5}	6.475×10^{-5}
P1	0.049	0.068	0.109	0.143	0.1875	0.196
P0	1.255	1.593	2.042	3.987	5.8690	6.173

Results

For this part of this research study, the efficiencies η, fill factors FF and the characteristic curves are the electrical properties of the PV panels that are being evaluated. It is planned to test c-Si and CIGS using the same methodology used in the literature (Akinoglu *et al*., 2021; Pastuszak and Węgierek, 2022; Imran *et al*., 2018).

Curves and Efficiencies

The two solar cells are tested under the same conditions with the same equipment under total illumination of the projector, at 115 W/m^2 of irradiance.

For each PV technology under study, a SEM analysis was done in order to observe surfaces with great detail. The result is presented in Fig. 10. Regarding the CIGS solar cell, as it can be seen in Fig. 10a, the SEM image is not fully clear on how many layers there are, but it is clearly possible to see the top encapsulating layer that appears to have a fabric-like texture, as it can be seen by the number of fibers. Concerning the silicon solar cell, presented in Fig. 10b, it is possible to detect clearly different layers. At the top, exits a type of oxide, due to the high presence of oxygen atoms, such as TCO (transparent conductive oxide) of the solar cell and, in the middle, there is a 225 μm crystalline silicon layer.

Figure 11 presents the obtained characteristics for both photovoltaic technologies. However, in order to compare both electrical properties of these solar cells, the effective area must be taken into consideration, since both cells have very distinctive sizes. Since it is not possible to determine directly the ISC for the CIGS PV panel, a linear regression is made to better determine the exact value of ISC per effective area.

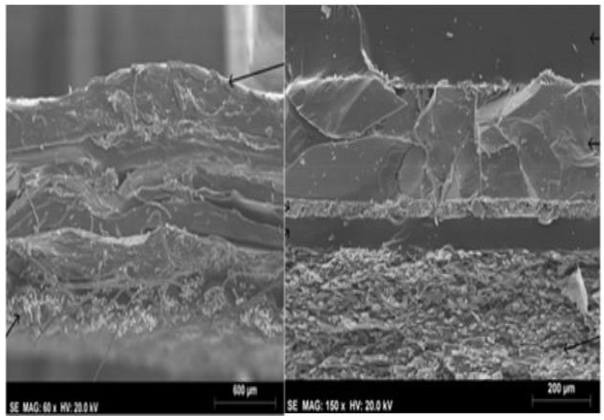

(a) CIGS solar cell (b) Silicon solar cell

Fig. 10: Cross-sectional SEM image for the two solar cells

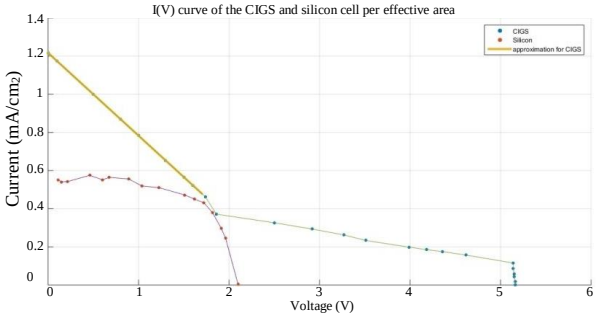

Fig. 11: I(V) curve for Silicon and CIGS per effective area

It is possible to Verify that the I(V) curve for silicon is very close to the ideal model of a solar cell (p-n junction model known as 1M3P). The deviation from the ideal model comes from the possible shunt resistance, R_{sh} or series resistance, Rs that are generated by imperfections of the layers or conduction losses of the connecting wires (De Melo Cunha *et al*., 2022; Song *et al*., 2021; Liu *et al*., 2020; Harrag and Messalti, 2017).

For 5.16 and 5 V, the CIGS panel's current rapidly increases at the huge slope, as it should be, compared to the ideal model. The curve of the cell is a bit more abrupt than the ideal model, but it could be caused by the heterojunction of different materials. This alludes to a possible internal low series resistance within the model because the series resistance is responsible for the region's slope. The higher the slope, the less influence will the series resistance, Rs, have on the circuit. From 5-2 V, the current is steadily increasing, contradicting the very slow increase and stabilization of the current at the ISC. Nevertheless, this behavior is not totally unrecognizable. When the shunt resistances of a solar cell are very low, there is an increase in the slope for this region, thereby enforcing the possibility of an internal shunt resistance within the CIGS solar cells. From 2-1.6 V, the slope increases drastically. At this point, the resistance of the load is at its minimum value (10 Ω). The only plausible explanation for this dramatic shift is given by M. Burgelman's study on CIGS material (Burgelman and Niemegeers, 1998). In this study, the author proved the existence of in-layer resistances that were formed during the fabrication process which could behave as shunt resistances. This resistance is formed naturally during fabrication, however since the CIGS solar panel under analysis is flexible, the fabrication process must have been different from regular rigid thin-film solar cells. Therefore, the shunt resistance effect was amplified (Burgelman and Niemegeers, 1998). From 1.6-0 V, there are no values shown. Still, with the previous conclusions, it is possible to assume that the linear behavior would remain identical and to better represent these results a linear regression was considered to determine the value of the ISC of the CIGS panel (Song *et al*., 2021; Liu *et al*., 2020; Harrag and Messalti, 2017).

Table 9 presents the electrical properties of both solar cells. It is possible to verify that the highest VOC and ISC per area are registered on the CIGS solar panel. An explanation for this could be the number of solar cells within the panel and their connection (series or parallel). Furthermore, the incident light spectrum is not constant as modeled in the simulations. This analysis will be carried out in the following sections. The crystalline silicon solar panel registered an efficiency value of 6.43% and a fill factor of 64.03%, as registered in Table 9. Moreover, the CIGS flexible panel achieved a higher efficiency than silicon, but its fill factor is drastically lower, since the "squareness" of the CIGS I(V) curve is far from the ideal one, i.e., the behavior of these heterojunctions is not described by a simple p-n junction model.

Light Absorption

In this section, each panel's responsivity is compared with the emission spectrum of the projector light. It is used the simulation results in order to achieve this comparison. This connection of parameters allows a better understanding of the performance of the solar panels.

The lighting projector used in the experiment is the Ersetze Jede Gebrochene Schutzscheibe R7s 500W max, composed of a halogen light bulb type (Guaix, 2015). Silicon's efficiency presented to be lower than the CIGS panel, but nonetheless, its FF proved that the main problem is related to the area of the cell. When the responsivity is crossed with the emission spectrum of the light projector, as illustrated in Fig. 12 it is possible to obtain some conclusions.

Moving on to CIGS, it is possible to verify from Figs. 13-15 that the absorption range of each cell is reduced as the gallium concentration increases. Furthermore, from the 200-400 nm region of the graph, it is possible to verify that little to zero radiation will be generated into current, due to the lack of light emission at that region, regardless of the concentration of gallium. From 450-900 nm, the light emission starts increasing and so does the CIGS responsivity. At this mark, the gallium concentration comes into action.

Table 9: Extracted electrical properties of the silicon and CIGS solar panels

Material	V_{OC} (V)	I_{SC} (mA/cm^2)	I_{max} (mA/cm^2)	V_{max} (V)	P_{max} (mW/cm^2)	FF (%)	η (%)
Silicon	2.10	0.552	0.4308	1.723	0.7422	64.03	6.43
CIGS	5.16	1.217	0.2625	3.270	0.8584	13.67	7.44

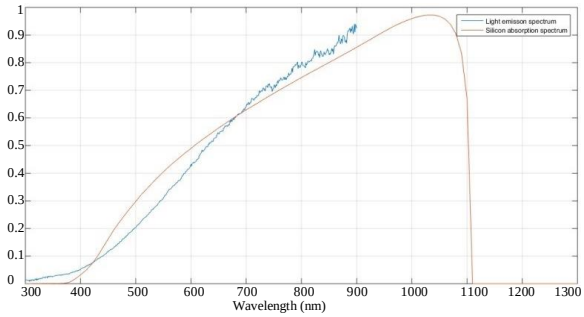

Fig. 12: Emission spectrum for the halogen light projector

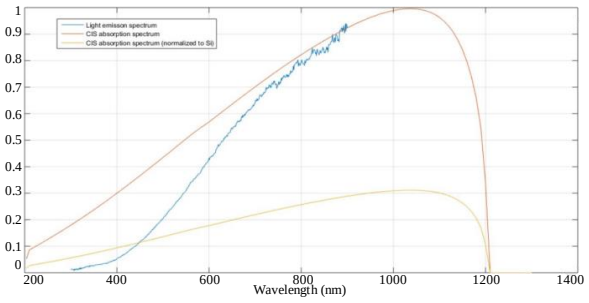

Fig. 13: Comparison of the light emission spectrum with CIS responsivity

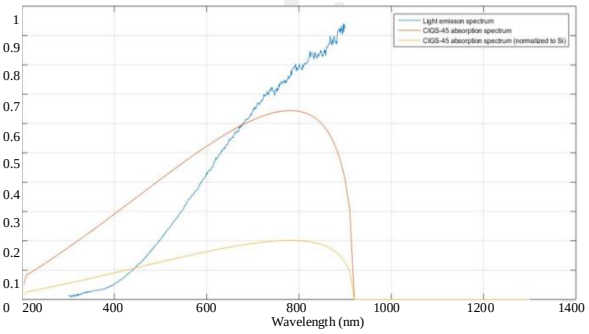

Fig. 14: Comparison of the light emission spectrum with CIGS-45 responsivity

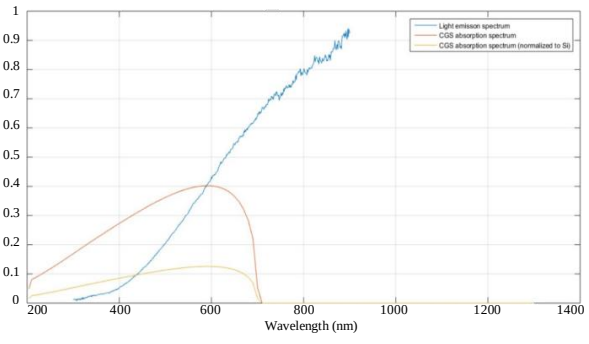

Fig. 15: Comparison of the light emission spectrum with CGS responsivity

Firstly, between 300 and 380 nm, silicon does not absorb any of the incident light, since this corresponds to the UV region. Even if it was inside the absorption spectrum of silicon, the amount of irradiated light would be very little, absorbing in both cases no UV radiation whatsoever.

For the 400 nm and for the 700 nm silicon's responsivity starts increasing at a fast pace, even surpassing the light projector's irradiation. The light emission also increases, but not as steeply as the silicon's responsivity at first. Nonetheless, radiation absorbed will be absorbed by the solar cell, since both functions are increasing and also because silicon has a very high current generation at this gap. Also, from 700-900 nm the light emission reaches its peak. Despite the silicon's responsivity peak at 1030 nm, the responsivity still circles 70% all the way up to 90% around the red and IR region. This shows how high the current can be generated in the silicon material for this particular light. However, the experimental results do not share the same statement, because the CIGS short circuit current per area is higher than silicon's.

In what concerns the CGS solar cell, the cell starts producing current at 710 nm, which means that only the visible spectrum will be absorbed by the cell and transformed into current. Thus, the current generation from the light will be very small since most of its highest wavelengths will pass through the cell or will be reflected, as the wavelengths that are encompassed in the responsivity of CGS, will produce a current equivalent to 40% of CIS maximum.

For the CIS solar cell, the highest peak in responsivity is located at 1060 nm, which implies that no light will reach the maximum current generation point. However, on this window, the maximum emission of the light projector is very close to the maximum absorption, which means that more current will be produced. The generated current will be high, but not as high as if it is compared to silicon's since it is much lower.

The CIGS-45 cell is the middle ground between the CGS and the CIS since its responsivity peak happens at 780 nm, having a value of about 60% of the CIS maximum and stops absorbing at 920 nm. This material can absorb throughout the whole emission spectrum of light, making it a good candidate for the assumption of the type of CIGS material.

Throughout this analysis, it is possible to assume that the panel used in the experiments does not contain a very large concentration of gallium since its absorption range is very short and does not match the experimental results. To solidify this statement, Isabela has proven that CIS can absorb 60% more IR radiation than CGS solar cells (Isabela *et al*., 2021).

VOC Analysis

T. Kirchartz and *U.* Rau in their study have investigated different models that use internal parameters of the solar cell (e.g., mobility carriers, band

gap, absorption coefficients) that can be used to obtain performance metrics of solar cells like the *VOC* (Kirchartz and Rau, 2018), using expression 2, where *k* corresponds to the Boltzmann's constant, *T* is the temperature, *q* is the module of the electron charge, *Eg* is the bandgap energy, *JSC* is the short-current density, *d* corresponds to the absorber layer thickness and *NC* and *NV* are the effective density of states of the conduction and valence band, respectively:

$$V_{OC}=2kT\ln\left(\frac{J_{SC}}{qd\frac{\sqrt{N_C N_V}}{2\pi}e^{\frac{-E_g}{2kT}}}+1\right) \quad (2)$$

In order to use this formula, some assumptions had to be made: (i) To use this equation, it is assumed that the absorbing layer of the solar cell is fully depleted; (ii) The internal values of the materials that were used are originated from the simulations; (iii) It is used the obtained ISC per effective area from the experimental results to replace the necessary short circuit current density. As previously stated, this assumption implies that the solar panels are composed of only one single solar cell, with the same area as the whole panel.

The experimental values are presented in Table 10. The VOC values are about 5.16 and 2.10 V for the CIGS and silicon solar panels, respectively, while the highest theoretical value for VOC is 1.252 and 0.704 V for the CIGS and silicon solar panels, respectively. This means that the solar panel cannot be represented by just one solar cell and there must be a series of n solar cells, in order to produce the experimental VOC values. This is why the third assumption is erroneous and does not entirely represent the actual reality, thus not being taken into consideration in the previous sections of the experiments. It is possible to determine the obtained VOC by comparing it with the experimental values. For silicon, it's possible to see that three solar cells generate the same voltage as the entire panel. For CIGS it is possible to check that the number of required cells decreases every time the gallium concentration is increased since the voltage gets higher. However, if the solar cells are all in series it is possible to assume that the concentration of the CIGS panel would be mainly indium. Still, it is a statement that cannot be entirely certified.

Table 10: New estimated values of VOC for different numbers of solar cells connected in series

Materials	Silicon	CIS	CIGS-31	CIGS-45	CIGS-66	CGS
VOC	0.704	0.512	0.712	0.832	0.972	1.252
Estimated # of cells	3.000	10.00	7.000	6.000	5.000	4.000
Estimated V_{OC}	2.112	5.12	4.984	4.992	4.86	5.008
Experimental V_{OC}	2.120	5.16	5.160	5.160	5.16	5.160

Conclusion

The main goal of this study is to compare some solar cells from different photovoltaic generations, like CIGS and silicon and compare some of their properties and parameters.

The 2D PIN model after being validated proved that there are some differences when assuming a CIGS solar cell as a PIN structure, although the shape and the absorption range of the CIGS solar cell are very similar to other studied solar cells of the same material. The main difference is located in the amount of generated current. Regardless, the obtained simulated results verify that CIGS can absorb to some extent some UV radiation and IR radiation, depending on the amount of Indium that is deposited in the fabrication of the cell. For the silicon solar cell, it is possible to see that the responsivity results were close to what they were expected as well. Being a simpler solar cell, it makes it easier to recreate it in software.

The relationship between the generated current and power proved that different materials would affect this characteristic. This analysis had the goal of capturing changes in the linear behavior between incident power and the generated current, so to better understand this, the poly fit function in MATLAB is used, in order to extract the polynomial expression that best fits the data. Silicon proved that first-generation materials (homojunction) have a linear relationship between current and power, but CIGS (a heterojunction) proved that the equation that best fitted the output data is a 3rd° polynomial expression. However, this non-linearity only proved true for regions other than the UV, where it remained linear, regardless of the gallium concentration.

Regarding real solar panels, the CIGS solar cell proved to have a very high short circuit current, since for the lowest value of load resistance, the voltage is not close to zero, proving the high illumination current that could be generated from the solar panel. The efficiency is relatively lower for a CIGS panel, but since this panel is made from a flexible substrate, naturally will achieve lower efficiencies than a rigid CIGS panel. Also, test conditions are not used to measure and certify the maximum efficiency of a solar cell (values presented in the introduction of this research work).

It is possible to notice the high impact that gallium has on this type of material since fewer concentrations of it will increase the short-circuit current but will cripple the open circuit voltage. So, depending on the desired application, CIGS can be designed to fit those needs. This type of versatility is almost impossible in a traditional silicon solar panel since there is no way of configuring beforehand how to refine the ISC or VOC values of the panel.

Acknowledgment

This study was supported in part by FCT/MCTES through national funds and in part by cofounded EU funds under project UIDB/EEA/50008/2020. Also, this study was supported by FCT under the research grant UI/BD/151091/2021.

Funding Information

The authors have not received any financial support or funding to report.

Author's Contributions

Afonso Ravasco: Conceptualization, software, methodology and formal analysis.

Ricardo A. Marques Lameirinhas and Catarina P. Correia V. Bernardo: Conceptualization, Written-reviewed and edited.

João Paulo N. Torres: Conceptualization, software, methodology, investigation, formal analysis and supervision.

Ethics

This article is original and contains unpublished material. The corresponding author confirms that all of the other authors have read and approved the manuscript and that no ethical issues are involved.

References

Akinoglu, B. G., Tuncel, B., & Badescu, V. (2021). Beyond 3rd generation solar cells and the full spectrum project. Recent advances and new emerging solar cells. *Sustainable Energy Technologies and Assessments*, *46*, 101287. https://doi.org/10.1016/j.seta.2021.101287

Alizade, R., & Ghadimi, A. (2019). The study of quantum efficiency in PIN photodiodes in terms of temperature and capacitive effects under non-uniform illumination conditions. *Optical and Quantum Electronics*, *51*, 1-14. https://doi.org/10.1007/s11082-018-1728-1

Amraoui, R., Aissat, A., Vilcot, J. P., & Decoster, D. (2022). Frequency response optimization of PIN photodiode based on in gaasn lattice matched to GaAs for high-speed photodetection applications. *Optics and Laser Technology*, *145*, 107468. https://doi.org/10.1016/j.optlastec.2021.107468

Battaglia, C., Cuevas, A., & De Wolf, S. (2016). High-efficiency crystalline silicon solar cells: Status and perspectives. *Energy and Environmental Science*, *9*(5), 1552-1576. https://doi.org/10.1039/C5EE03380B

Burgelman, M., & Niemegeers, A. (1998). Calculation of CIS and CdTe module efficiencies. *Solar Energy Materials and Solar Cells*, *51*(2), 129-143. https://doi.org/10.1016/S0927-0248(97)00227-4

De Melo Cunha, J. P., Marques Lameirinhas, R. A., & N. Torres, J. P. (2022). Multi-junction solar cells and nanoantennas. *Nanomaterials*, *12*(18), 3173. https://doi.org/10.3390/nano12183173

Dos Santos Castilho, C., N. Torres, J. P., Ferreira Fernandes, C. A., & Marques Lameirinhas, R. A. (2021). Study on the implementation of a solar photovoltaic system with self-consumption in an educational building. *Energies*, *14*(8), 2214. https://doi.org/10.3390/en14082214

Harrag, A., & Messalti, S. (2017). Three, five and seven PV model parameters extraction using PSO. *Energy Procedia*, *119*, 767-774. https://doi.org/10.1016/j.egypro.2017.07.104

Imran, J. Jiang, D. Eric, M. Zahid, & Yousaf, M. (2018). Parametric optimization of gaas pin solar cell. *08*. https://www.researchgate.net/publication/327338351_Parametric_optimization_of_GaAs_PIN_Solar_Cell

Isabela, C. B., Lameirinhas, R. A. M., Torres, J. P. N., & Fernandes, C. A. (2021). Comparative study of the Copper Indium Gallium Selenide (CIGS) solar cell with other solar technologies. *Sustainable Energy and Fuels*, *5*(8), 2273-2283. https://doi.org/10.1039/D0SE01717E

Jalali, H., Orouji, A. A., & Gharibshahian, I. (2023). Controlled conduction band offset in Sb2Se3 solar cell through introduction of (Zn, Sn) O buffer layer to improve photovoltaic performance: A simulation study. *Solar Energy Materials and Solar Cells*, *260*, 112492. https://doi.org/10.1016/j.solmat.2023.112492

Kant, N., & Singh, P. (2022). Review of next generation photovoltaic solar cell technology and comparative materialistic development. *Materials Today: Proceedings*, *56*, 3460-3470. https://doi.org/10.1016/j.matpr.2021.11.116

Kirchartz, T., & Rau, U. (2018). What makes a good solar cell?. *Advanced Energy Materials*, *8*(28), 1703385. https://doi.org/10.1002/aenm.201703385

Guaix (2015). Spectra of Lamps. https://guaix.fis.ucm.es/lamps_spectra

Layachi, O. A., Azmi, S., Moujib, A., Nohair, M., & Khoumri, E. L. (2023). Investigation of nucleation and growth mechanism of Cu2ZnSnS4 absorber layer electrodeposition on Indium tin oxide coated glass. *Thin Solid Films*, *782*, 140019. https://doi.org/10.1016/j.tsf.2023.140019

Liu, Y., Li, Y., Wu, Y., Yang, G., Mazzarella, L., Procel-Moya, P., ... & Sun, B. (2020). High-efficiency silicon heterojunction solar cells: Materials, devices and applications. *Materials Science and Engineering: R: Reports*, *142*, 100579. https://doi.org/10.1016/j.mser.2020.100579

Marques Lameirinhas, R. A., Torres, J. P. N., & de Melo Cunha, J. P. (2022). A photovoltaic technology review: history, fundamentals and applications. *Energies*, *15*(5), 1823. https://doi.org/10.3390/en15051823

Nain, P., & Kumar, A. (2021). Theoretical evaluation of metal release potential of emerging third generation solar photovoltaics. *Solar Energy Materials and Solar Cells*, *227*, 111120. https://doi.org/10.1016/j.solmat.2021.111120

Nicolás-Marín, M. M., González-Castillo, J. R., Vigil-Galán, O., & Courel, M. (2022). The state of the art of Sb2 (S, Se) 3 thin film solar cells: current progress and future prospect. *Journal of Physics D: Applied Physics*, *55*(30), 303001. https://doi.org/10.1088/1361-6463/ac5f32

Olchowik, W., Bednarek, M., Dąbrowski, T., & Rosiński, A. (2023). Application of the energy efficiency mathematical model to diagnose photovoltaic micro-systems. *Energies*, *16*(18), 6746. https://doi.org/10.3390/en16186746

Palit, S., & Hussain, C. M. (2018). Engineered nanomaterial for industrial use. *In Handbook of Nanomaterials for Industrial Applications*, 3-12. Elsevier. https://doi.org/10.1016/B978-0-12-813351-4.00001-8

Pastuszak, J., & Węgierek, P. (2022). Photovoltaic cell generations and current research directions for their development. *Materials*, *15*(16), 5542. https://doi.org/10.3390/ma15165542

Paulson, P. D., Birkmire, R. W., & Shafarman, W. N. (2003). Optical characterization of CuIn 1-x Ga x Se 2 alloy thin films by spectroscopic ellipsometry. *Journal of Applied Physics*, *94*(2), 879-888. https://doi.org/10.1063/1.1581345

Pinho Correia Valério Bernardo, C., Marques Lameirinhas, R. A., Neto Torres, J. P., & Baptista, A. (2023). The shading influence on the economic viability of a real photovoltaic system project. *Energies*, *16*(6), 2672. https://doi.org/10.3390/en16062672

Soga, T. (Ed.). (2006). *Nanostructured Materials for Solar Energy Conversion*. Elsevier. https://doi.org/10.1016/B978-044452844-5/50002-0

Song, Z., Fang, K., Sun, X., Liang, Y., Lin, W., Xu, C., ... & Yu, F. (2021). An effective method to accurately extract the parameters of single diode model of solar cells. *Nanomaterials*, *11*(10), 2615. https://doi.org/10.3390/nano11102615

Sun, C., Zou, Y., Qin, C., Zhang, B., & Wu, X. (2022). Temperature effect of photovoltaic cells: A review. *Advanced Composites and Hybrid Materials*, *5*(4), 2675-2699. https://doi.org/10.1007/s42114-022-00533-z

Torres, J. P. N., Marques Lameirinhas, R. A., Pinho Correia Valério Bernardo, C., Lima Martins, S., Mendonça dos Santos, P., Veiga, H. I., ... & Santos do Rego Figueiredo, P. M. (2023a). Analysis of different third-generation solar cells using the discrete electrical model d1mxp. *Energies*, *16*(7), 3289. https://doi.org/10.3390/en16073289

Torres, J. P. N., Marques Lameirinhas, R. A., Correia V. Bernardo, C. P., Veiga, H. I., & dos Santos, P. M. (2023b). A discrete electrical model for photovoltaic solar cells-d1MxP. *Energies*, *16*(4), 2018. https://doi.org/10.3390/en16042018